

TI Designs Fluxgate-Based Displacement Sensor



TI Designs

The TIDA-00463 showcases a displacement sensor for linear distance measurements in a BoosterPack™ form factor for TI LaunchPad™.

The design is suitable for any application where a distance measurement, even through non-magnetic materials, is needed and non-contact, wear-free measurements are required.

Through the use of magnetic fluxgate technology, this design is able to cover a wide measurement distance while achieving high resolution and accuracy.

Design Resources

[TIDA-00463](#)

Tool Folder Containing Design Files

[DRV425](#)

Product Folder

[ADS1248](#)

Product Folder

[TPS71745](#)

Product Folder

Design Features

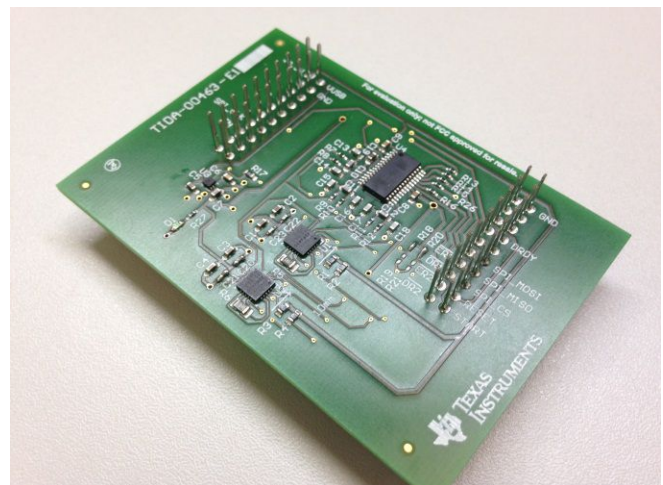
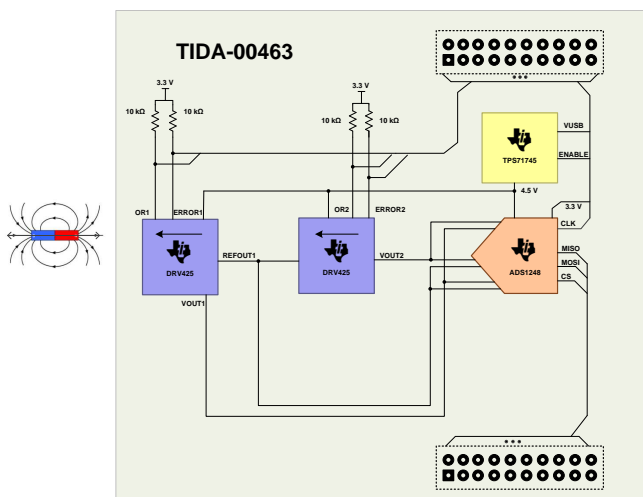
- Measures 10-cm Distance, 1-mm Resolution With a 6-mm diameter NdFeB Magnet ($H_C > 1350$ kA/m)
- Detects the Presence of the Magnet up to 30 cm
- Common Mode Fields Rejection
- Temperature Range: -40°C to 125°C
- No Temperature Dependence:
Max Temp Drift = 100 nT/ $^{\circ}\text{C}$
- Non-Contact, Wear-Free Measurements
- Detects Even Through Non-Magnetic Materials
- BoosterPack Form Factor, Compatible With TI LaunchPad

Featured Applications

- Factory Automation and Process Control
- Sensors And Field Transmitters
- Robotics



[ASK Our E2E Experts](#)



An IMPORTANT NOTICE at the end of this TI reference design addresses authorized use, intellectual property matters and other important disclaimers and information.

All trademarks are the property of their respective owners.

1 Key System Specifications

The following parameters depend on the magnet used in the application. For the TIDA-00463, the chosen magnet (NdFeB) has a diameter of 6 mm and a $H_C > 1350$ kA/m.

Table 1. System Parameters

PARAMETER	SPECIFICATION	DETAILS
Max detectable distance	30 cm	See Section 7.1
Resolution	1 mm (from 2 to 10 cm)	See Section 7.1
Response time	Dependent from ADC data rate	See Section 3.6.2
CM fields rejection		See Section 3.5
Noise (peak-to-peak)	320 nT	See Section 7
Temperature	-40°C to 125°C	See Section 3.6.3
Max temp drift	100 nT/°C	See Section 7.3
Supply voltage	4.5 V	See Section 3.6.3

2 System Description

This design is meant for contactless magnetic-based linear distance measurement using fluxgate technology integrated in the DRV425.

The TIDA-00463 eliminates big common mode field interferences (for example, the earth magnetic field) thanks to the adopted differential approach where the outputs of the two sensors are measured differentially. Nevertheless, it is possible to measure the output of each sensor independently being able to estimate as well, if present, any common mode field.

The solution is available in a BoosterPack form factor and compatible with TI LaunchPad to easily use and evaluate.

3 System Design Theory

The system is designed for linear distance measurements where the distance is dependent on the magnetic field generated by any magnet. The measured distance depends on the strength and dimension of the magnet, stronger is the magnet bigger is the distance that the sensor is able to measure.

The used sensor is the DRV425, which provides the unique and proprietary, integrated fluxgate sensor (IFG) with an internal compensation coil to support a high-accuracy sensing range of ± 2 mT with a measurement of up to 47 kHz.

3.1 Magnetic Sensors

Magnetic field strength is measured using a variety of technologies. Each technique has unique properties that make it more suitable for particular applications. A magnetic field is one of the most important physical quantities that have been used in many applications such as: research of magnetic materials, geophysics, space, navigation system (detecting wafting goods), mapping of earth's magnetic field, electronic compass, determination of object's position or sensor apart in small order, and many other applications [1] [2]. These applications can range from simple sensing to precise measurements of a magnetic field. Based on magnetic field strengths and measurement range, magnetic field sensors can be divided into two categories:

1. Sensors that measure low fields (< 1 mT), commonly called magnetometers
2. Sensors that measure high fields (> 1 mT), commonly called Gauss meters [3]

Magnetometers can be divided into vector component and scalar magnitude types. Vector magnetometers measure the vector components of a magnetic field while scalar magnetometers measure the magnitude of the vector magnetic field.

3.2 Fluxgate Technology

The heart of a fluxgate magnetometer is the fluxgate. It is the transducer that converts magnetic field into electric voltage. The fluxgate is the most widely used magnetic field vector measuring instrument. It is rugged, reliable, and relatively less expensive than the other low-field vector measuring instruments. These characteristics, along with its ability to measure the vector components of magnetic fields over a 0.1-nT to 1-mT range from DC to several kHz, make it a very versatile instrument.

Geologists use them to explore, and geophysicists use them to study the geomagnetic field (about 20 to 75 μ T on the Earth's surface). Satellite engineers use them to determine and control the attitude of spacecraft, scientists use them in their research, and the military uses them in many applications, including mine detection, vehicle detection, and target recognition. Some airport security systems use them to detect weapons [2] [3].

3.2.1 Electromagnet Principle

The fluxgate main principle uses a conductor, which carries the current of interest. The current generates a magnetic field; through this magnetic field measured by the device, it is possible to calculate the current flowing in the conductor.

Using Faraday's law of induction, where the induced EMF $\sim dB/dt$, estimate the changing (AC) current using a secondary winding (transformer); to measure the constant field, the user needs a magnetic sensor.

$$B = \frac{\mu_0 \times \mu_r \times I}{2 \times \pi \times R} \tag{1}$$

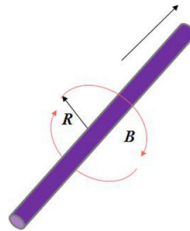


Figure 1. Ampere's Law (Also Applies to DC Currents)

3.2.2 General Mode of Operation

The fluxgate magnetometer consists of a ferromagnetic material core with two coils, an excitation, and a sense coil (see Figure 2). It exploits magnetic induction together with the fact that all ferromagnetic material becomes saturated at high fields. This saturation can be seen in the hysteresis loops shown on the right side of Figure 2 [4].

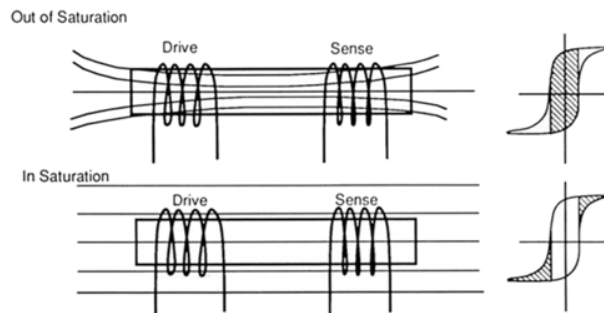


Figure 2. Illustration of Operating Principles of Fluxgate Magnetometers

NOTE: The output signal becomes modulated by driving the soft magnetic core into and out of saturation. The shaded regions indicate the regions of operation.

The core is magnetically saturated alternatively in opposing directions along any suitable axis by means of the excitation coil driven by a sine or square waveform. Prior to saturation, the ambient field is channeled through the core producing a high flux due to its high permeability. At the point of saturation, the core permeability falls away to the vacuum, causing the flux to collapse. During the next half cycle of the excitation waveform, the core recovers from saturation, and the flux due to the ambient field is once again at a high level until the core saturates in the opposite direction; the cycle then repeats [5].

The voltage output from the sense coil consists of even-numbered harmonics of the excitation frequency. For readout, the second harmonic is extracted and rectified. The voltage associated with this harmonic is proportional to the external magnetic field [4].

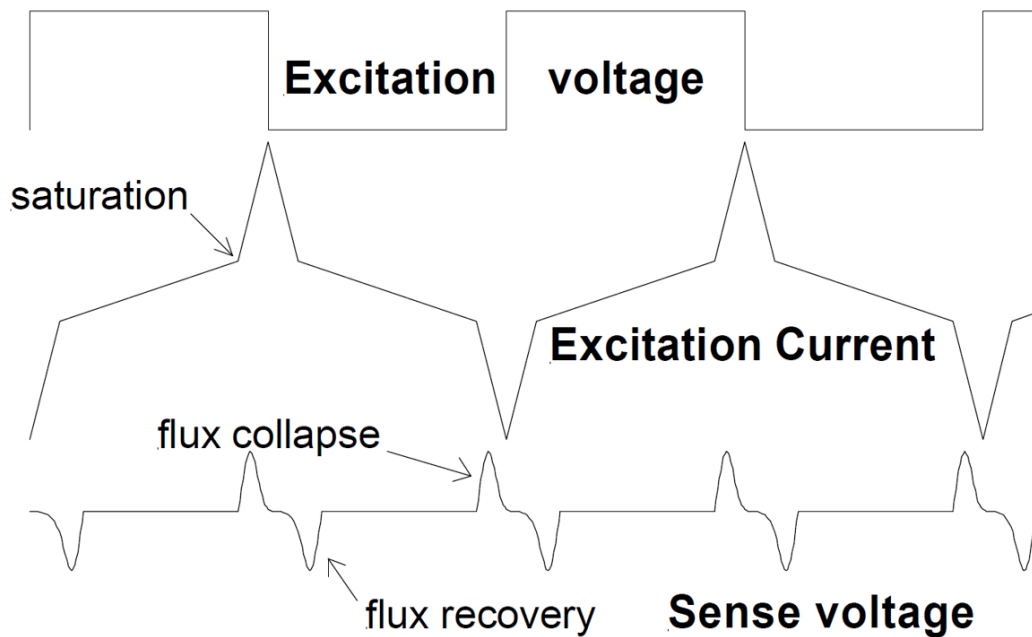


Figure 3. Ideal Fluxgate Waveforms

3.2.3 Saturation

Saturation is a state reached when an increase in applied magnetizing field H cannot increase the magnetization of the material further, so the total magnetic field B levels off. As the H field increases, the B field approaches a maximum value asymptotically, the saturation level for the substance. The magnetic field represents the existing current through a conductor. From this idea, the excited saturable inductor is able to measure current.

The saturation point of ferromagnetic materials depends on magnetic permeability and also depends on the amount of current. The core permeability will change both by an external field (produced by external current IPRIM) and an excitation current (IEXCT) through the inductor [6].

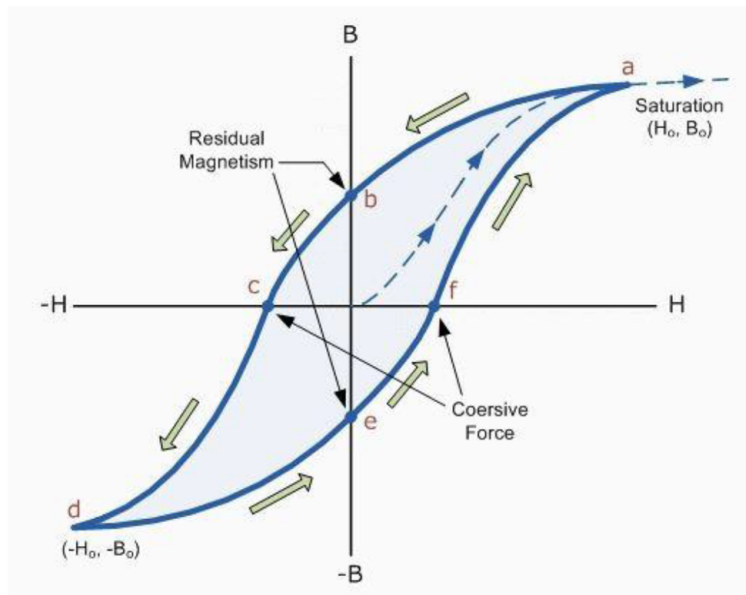


Figure 4. Magnetization Curve and B-H Curve

3.3 Specifics for Disc Magnets

The static magnetic field of a disc magnet is dependent on its magnetic remanence B_r , height h , and radius r . The magnetic flux density at a certain distance z from the surface of the magnet is calculated to

$$B(z) = \frac{B_r}{2} \left[\frac{h+z}{\sqrt{r^2 + (h+z)^2}} - \frac{z}{\sqrt{r^2 + z^2}} \right] \quad (2)$$

where

- B_r is the magnetic remanence
- h is the height
- r the radius of the disc magnet

The magnetic field strength is equal for both distances in either direction of the disc magnet. Only the magnetic field lines are orientated oppositely. Depending on the orientation of the magnet, compared to the electric field inside the conductor, the measured voltage is either of positive or negative sign.

3.4 Simulating Magnetic Field for System Design

Though many tools can be used to simulate magnetic field, this section details using the tool called FEMM 4.2 [6]. This tool uses the finite element method to calculate magnetic fields. The finite element method is a numerical method to calculate solutions for partial differential equations. In principle, the area in which the magnetic field is propagating is divided into several small elements with finite size. For every element, a basic function is defined. Together with boundary and transition conditions, these basic functions are inserted into the general partial differential equation. Then, the resulting system of equations is solved numerically. A detailed equation about the finite element method can be found in The Finite Element Method [7]. To explain the handling of the tool, see Figure 5. FEMM 4.2 calculates the magnetic field for axis symmetric objects, the y axis serves as rotation axis. A complete documentation of the tool can be found online at www.femm.info.

Follow these tips on how to run a FEMM 4.2 simulation if the user is not familiar with it:

- Define the dimensions of the magnet and its surrounding area. The box in the middle on the enlarged part of Figure 5 is the magnet, the outer area is air. The magnet has a diameter of 6 mm and a height of 5 mm.
- Set the properties of the defined areas. In this case, the orientation of the magnetization direction is set to 90° and the coercive field strength H_c is set to 1350 kA/m.
- For the surrounding area, specify as property the air. It is best practice to define a rectangular area (property: air) in the same direction the user wants to calculate the magnetic field.
- Now, simulate the magnetic field.

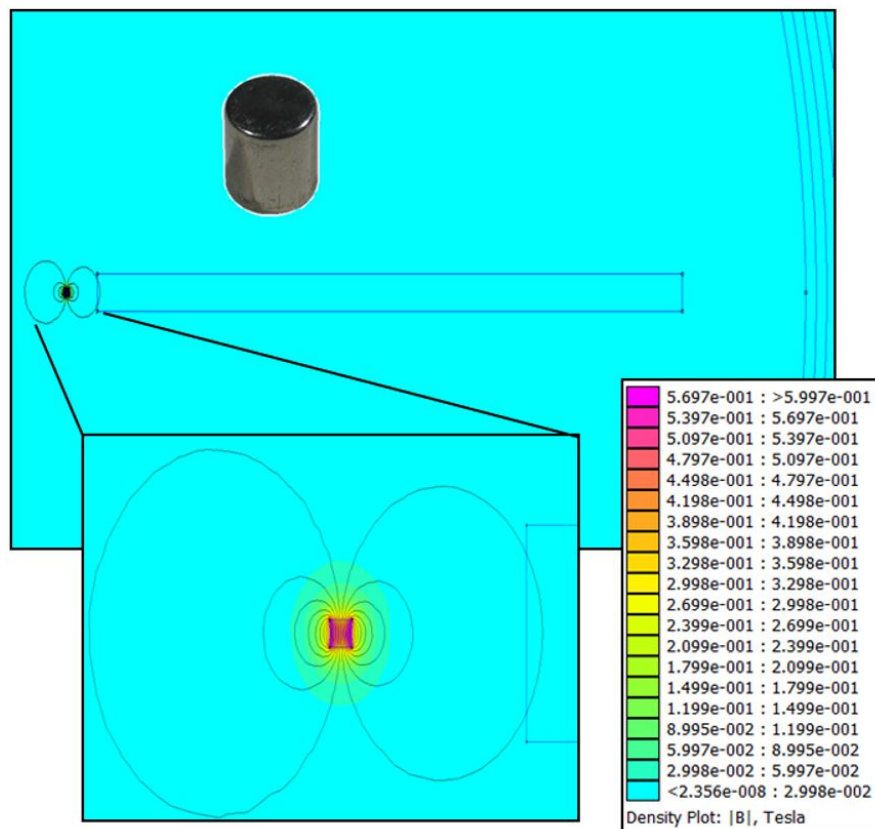


Figure 5. FEMM Simulation

The result is shown in Figure 5. The thin lines indicate the magnetic flux lines. The higher the density of the magnetic flux lines, the higher the magnetic flux density. In addition, this relation is also pointed out by different colors. Magenta indicates a high magnetic flux density, and cyan indicates a low magnetic flux density.

Furthermore, the tool can display the strength of the magnetic flux density along a user defined line. Therefore, a 1-m long line, from left to right perpendicular to the cross section of the magnet is drawn. The resulting curve is shown in Figure 6. The picture on the right side is an enlarged version of the one on the left.

Considering that the sensitivity of the DRV425 is 12.2 mA/mT with a shunt resistance of 20 Ω and a bandwidth setting equal to 0, the bandwidth of the sensor is equal to 30.738 kHz, meaning a noise density of 263 nT. This means that our sensor with this magnet, in absence of other magnetic sources, can measure up to a 1-m distance.

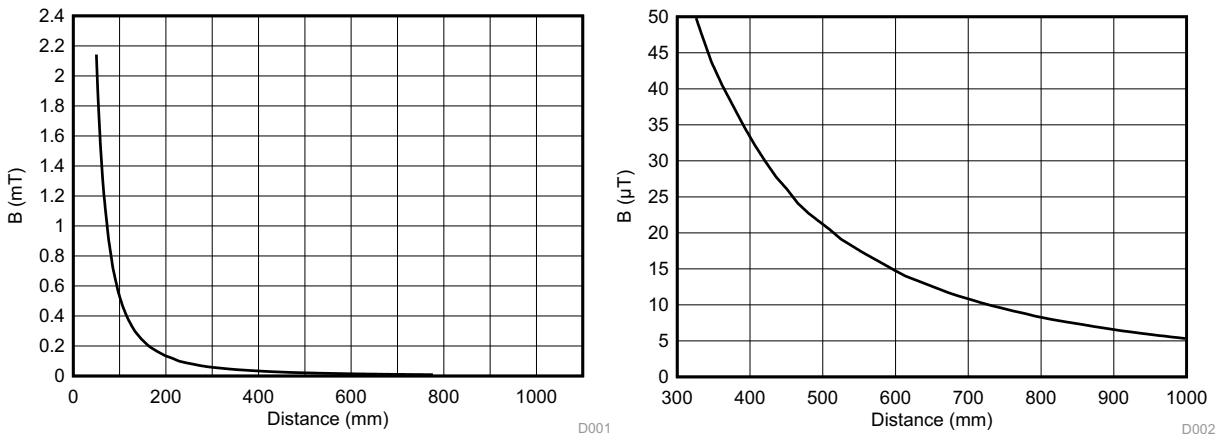


Figure 6. Magnetic Flux Density versus Distance

3.5 Differential Measurements

Under certain conditions, the DRV425 can measure up to hundreds of nT. However, considering that the earth magnetic field is in the range between 25 and 65 μT, the high sensitivity of the sensor becomes useless if the user does not calibrate before using.

In addition, the user should calibrate the system periodically because the earth magnetic field varies with time and with respect to the position of the system. Calibration requires additional time and resources.

To avoid calibration, the TIDA-00463 uses two DRV425 and measures the difference of the two outputs. The drawback of this solution is that the distance range is smaller with respect to the solution where only one sensor is used because information is given by the difference of the two voltage outputs: the closer the sensors are, the smaller the difference of the two voltage outputs and the measured distance become.

On the contrary, if the two sensors are far from each other, the common mode field influences detected by the two could not be anymore the same. Therefore, they will not be completely cancelled.

For the TIDA-00463, it was found that a good compromise in terms of distance between the two sensors is 10 mm. For differential measurements, the direction of the two sensors should be the same so that the common mode fields will cancel out.

Finally, the TIDA-00463 can measure the single output of the sensors to monitor the common mode fields.

3.6 Analog Signal Chain

3.6.1 Magnetic Field Sensing

The DRV425 is chosen because of its high sensitivity to any magnetic field that can measure bigger distances with respect to any other magnetic technology.

In addition the low offset, offset drift, and noise of the sensor, combined with the precise gain, low gain drift, and very low nonlinearity provided by the internal compensation coil, result in unrivaled magnetic field measurement precision.

Furthermore, it offers a complete set of features, including an internal difference amplifier, on-chip precision reference, and diagnostic functions to minimize component count and system-level cost.

The following procedure was used to design a solution for a linear-position sensor:

- Select the proper supply voltage (VDD) to support the desired magnetic field range (see [Table 2](#)).
- Select the proper reference voltage (V_{REFIN}) to support the desired magnetic field range and to match the input voltage specifications of the desired ADC.
- Use the DRV425 System Parameter Calculator, ([SLOC331](#); RangeCalculator tab) to select the proper shunt resistor value of R_{SHUNT} .
- The sensitivity drift performance of a DRV425-based linear position sensor is dominated by the temperature coefficient of the external shunt resistor. Select a low-drift shunt resistor for best sensor performance.
- Use the DRV425 System Parameter Calculator (Problems Detected Table in DRV425 System Parameters tab) to verify the system response.

The TIDA-00463 allows the user to read back the error and over-range flag of the two sensors, reading them back through the LaunchPad.

Table 2. Design Parameters

DESIGN PARAMETER	EXAMPLE VALUE
Magnetic field range	VDD = 5 V: ± 2 mT (max) VDD = 3.3 V: ± 1.3 mT (max)
Supply voltage, VDD	3.0 to 5.5 V
Reference voltage, V_{REFIN}	Range: GND to VDD If an internal reference is used: 2.5 V, 1.65 V, or VDD / 2
Shunt resistor, R_{SHUNT}	Depends on the desired magnetic field range, reference, and supply voltage; see the DRV425 Systems Parameter Calculator (SLOC331) for details.

Figure 7 shows the parameters selected for the TIDA-00463.



DRV425 - System Parameter Calculator

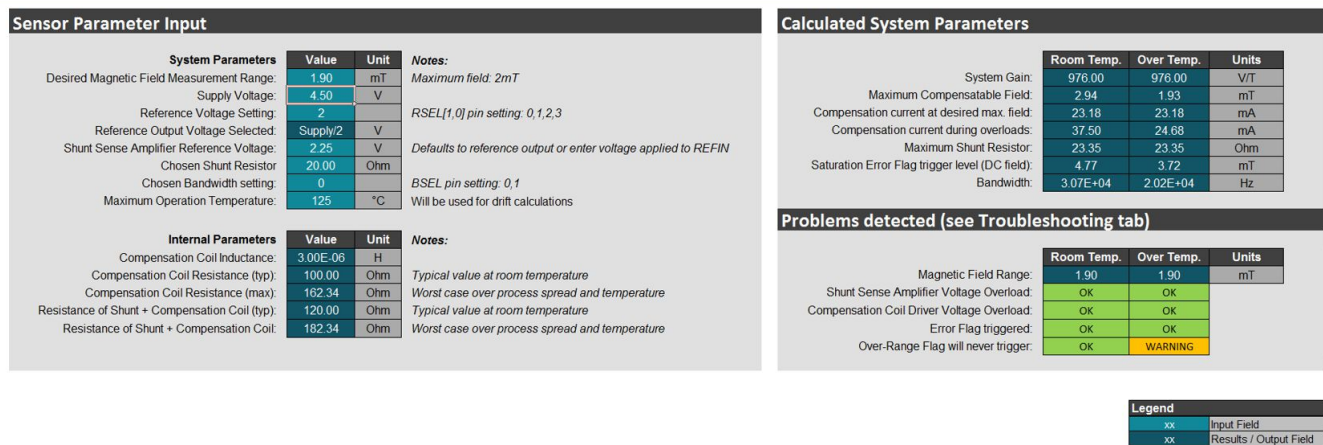


Figure 7. TIDA00-463 System Parameters

The maximum measurable magnetic field is 1.9 mT and system bandwidth is around 30 kHz. The tool detects only a warning over temperature related to the over-range flag, which it might not trigger. However, this is only a warning and it disappears if the max temperature is equal to 85°C. The output of the sensor is directly proportional to the measured magnetic field and it is calculated using Equation 3:

$$V_{OUT} = B \times G \times R_{SHUNT} \times G_{AMP} \tag{3}$$

where:

- B is the measured magnetic field
- G = 4 is the gain of the integrated differential amplifier
- R_{SHUNT} = 20 Ω is the external shunt resistor
- G = 12.2 mA/mT is the sensor gain

Substituting these values to Equation 3:

$$V_{OUT} = B \times 976 \frac{mV}{mT}$$

Considering that the maximum measurable magnetic field is 1.9 mT, the maximum measurable voltage output is 1.85 V.

3.6.2 Analog-to-Digital Conversion

For the TIDA-00463, the ADC needs to have the following requirements:

- ≥ 16 -bit ENOB
- \geq Three differential inputs
- 4.5-V analog supply
- 3.3-V digital supply
- Operating temperature: -40°C to 125°C

On TI's portfolio, the ADC that satisfies those requirements is the ADS1248, a precision 24-bit Sigma Delta ADC.

The ADS1248 can have an external reference voltage or an internal one. For the TIDA-00463, the chosen reference voltage for the ADS1248 is the internal one (2.048 V) because it has very low noise ($6\ \mu\text{V}_{\text{PP}}$) and a very low drift ($10\ \text{ppm}/^{\circ}\text{C}$).

In addition, 2.048 V covers all the signal range ($V_{\text{OUTMAX}}[\text{V}] = 1.85\ \text{V}$) and the LSB, considering ENOB = 16 bits, is equal to $31.25\ \mu\text{V}$, meaning $32\ \text{nT}$ is the minimum measurable magnetic field. Considering the ADS1248 datasheet, to achieve a 16-bit ENOB with AVDD = 4.5 V, AVSS = 0 V, internal reference = 2.048 V, and PGA = 1, the data rate has to be a maximum of 40 SPS. This limits the response time of the system because the DRV425 has a much higher bandwidth (30 kHz).

Also keep in mind that the common-mode input (V_{CMI}) must be within the range shown in [Equation 4](#):

$$\left(\text{AVSS} + 0.1\ \text{V} + \frac{V_{\text{IN}} \times \text{Gain}}{2} \right) \leq V_{\text{CMI}} \leq \left(\text{AVDD} - 0.1\ \text{V} - \frac{V_{\text{IN}} \times \text{Gain}}{2} \right) \quad (4)$$

For the TIDA-00463, $1.025\ \text{V} \leq V_{\text{CMI}} \leq 3.475\ \text{V}$, where V_{CMI} is around 1.32 V. At the input of each differential channel, an antialiasing filter is present to reduce the differential and common-mode noise.

The ADS1248 sends out the data to the LaunchPad and is configured by this one through SPI.

3.6.3 Board Power Supply

The TIDA-00463 is powered by the TPS71745, a single-output LDO with a fixed voltage equal to 4.5 V. The input voltage of the TPS71745 is the USB voltage coming directly from the LaunchPad equal to $5\ \text{V} \pm 0.25\ \text{V}$. Considering a minimum input voltage equal to 4.75 V, the TPS71745 assures at the output a voltage equal to 4.5 V with which the entire board can be powered through to the 150-mA output current provided by it.

One of the other reasons why the TPS71745 is selected is for its temperature range that goes from -40°C to 125°C , which aligns with the other ICs temperature range, making the entire board temperature range between -40°C and 125°C .

The current consumption of the TIDA-00463 is around 20 mA; in low power systems, a duty cycle control of the board power supply could lower the TIDA-00463 current consumption. The enable pin, controlled by the LaunchPad, on the TPS71745 allows to do that. The TPS71745 also has low noise ($30\ \mu\text{V}_{\text{RMS}}$ typical) and high bandwidth PSRR.

Do not use a converter because the current flowing on the external inductor generates a magnetic field that could influence the measurements.

4 Block Diagram

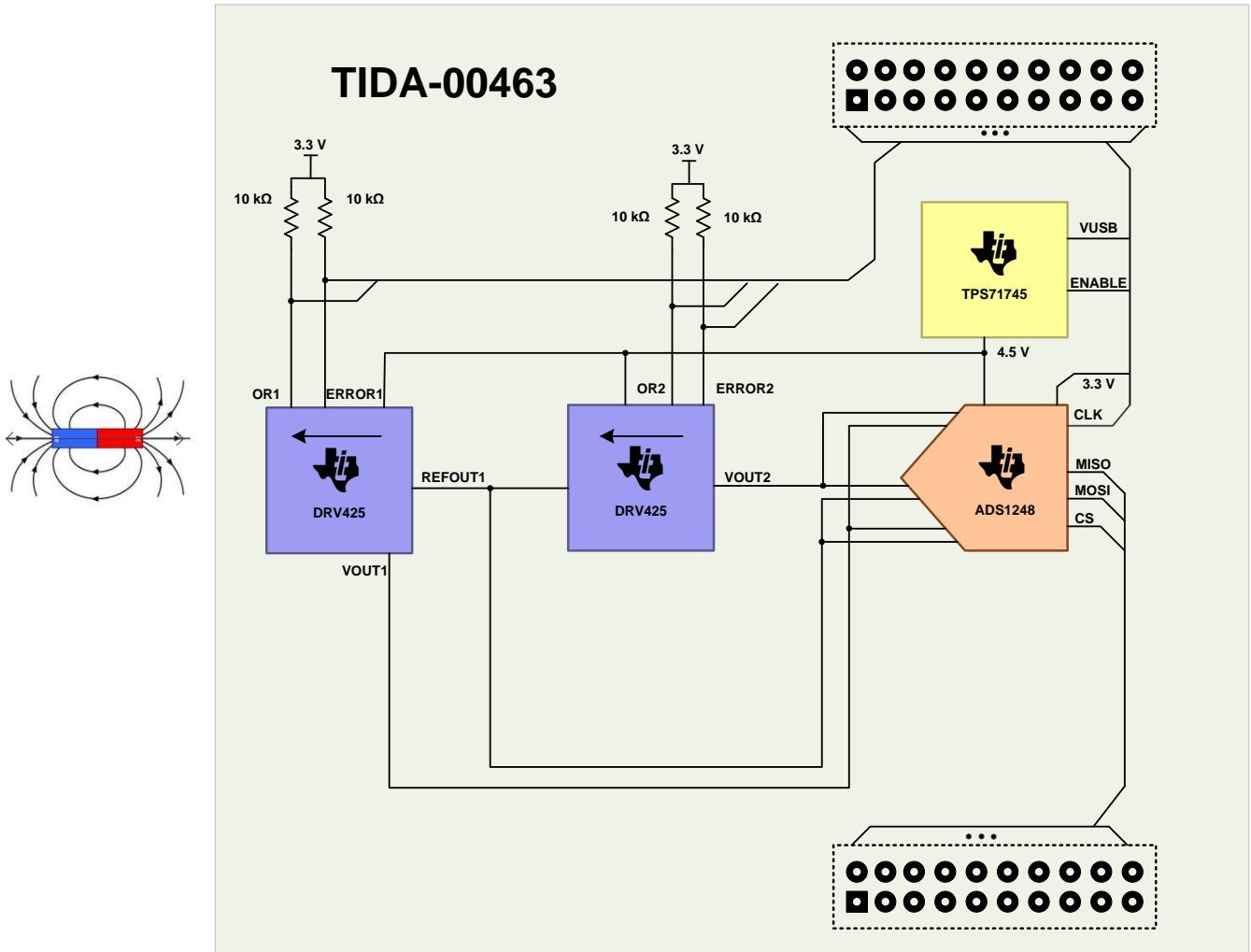


Figure 8. TIDA-00463 Block Diagram

4.1 Highlighted Products

For more information on each of these devices, see their respective product folders at www.ti.com.

4.1.1 DRV425—Fluxgate Magnetic Field Sensor

Features:

- High-precision, integrated fluxgate sensor:
 - Offset: $\pm 8 \mu\text{T}$ (Max)
 - Offset drift: $\pm 5 \text{ nT}/^\circ\text{C}$ (Typ)
 - Gain error: 0.04% (Typ)
 - Gain drift: $\pm 7 \text{ ppm}/^\circ\text{C}$ (Typ)
 - Linearity: $\pm 0.1\%$
 - Noise: $1.5 \text{ nT}/\sqrt{\text{Hz}}$ (Typ)
- Sensor range: $\pm 2 \text{ mT}$ (Max)
 - Range and gain adjustable with external resistor
- Selectable bandwidth: 47 or 32 kHz
- Precision reference:
 - Accuracy: 2% (max); Drift: 50 ppm/ $^\circ\text{C}$ (max)
 - Pin-selectable voltage: 2.5 or 1.65 V
 - Selectable ratiometric mode: $V_{\text{DD}} / 2$
- Diagnostic features: Overrange and error flags
- Supply voltage range: 3.0 to 5.5 V

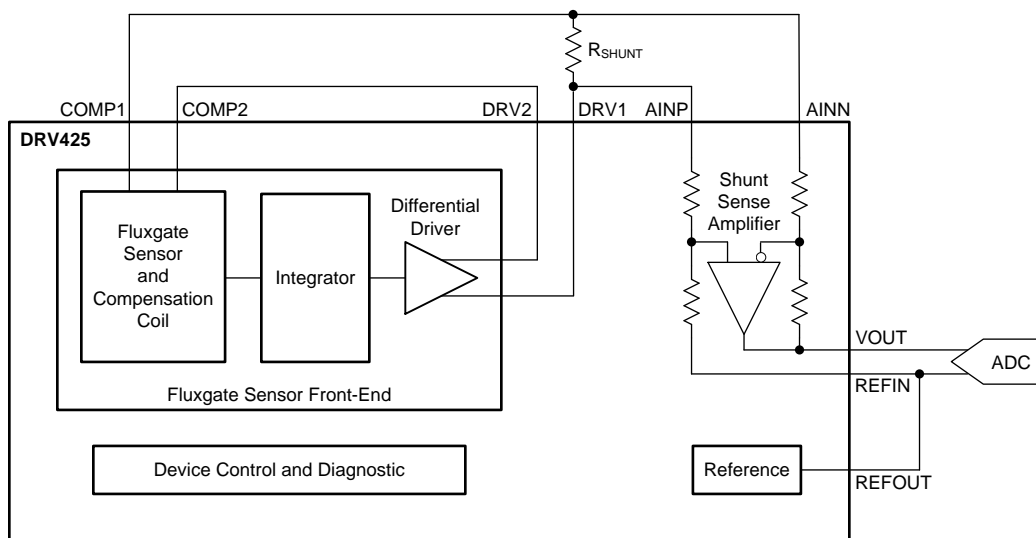


Figure 9. DRV425 Simplified Schematic

4.1.2 ADS1248—Precision 24-Bit ADC

Features:

- Data output rates up to 2 kSPS
- Single-cycle settling for all data rates
- Simultaneous 50- and 60-Hz rejection at 20 SPS
- Four differential, seven single-ended inputs (ADS1248)
- Low-noise PGA: 48 nV_{RMS} at PGA = 128
- Matched current source DACs
- Very low drift internal voltage reference: 10 ppm/°C (maximum)
- Sensor burn-out detection
- Eight general-purpose I/Os
- Internal temperature sensor
- Power supply and V_{REF} monitoring (ADS1247, ADS1248)
- Self and system calibration
- SPI-compatible serial interface
- Analog supply unipolar (2.7 to 5.25 V) and bipolar (±2.5 V) operation
- Digital supply: 2.7 to 5.25 V

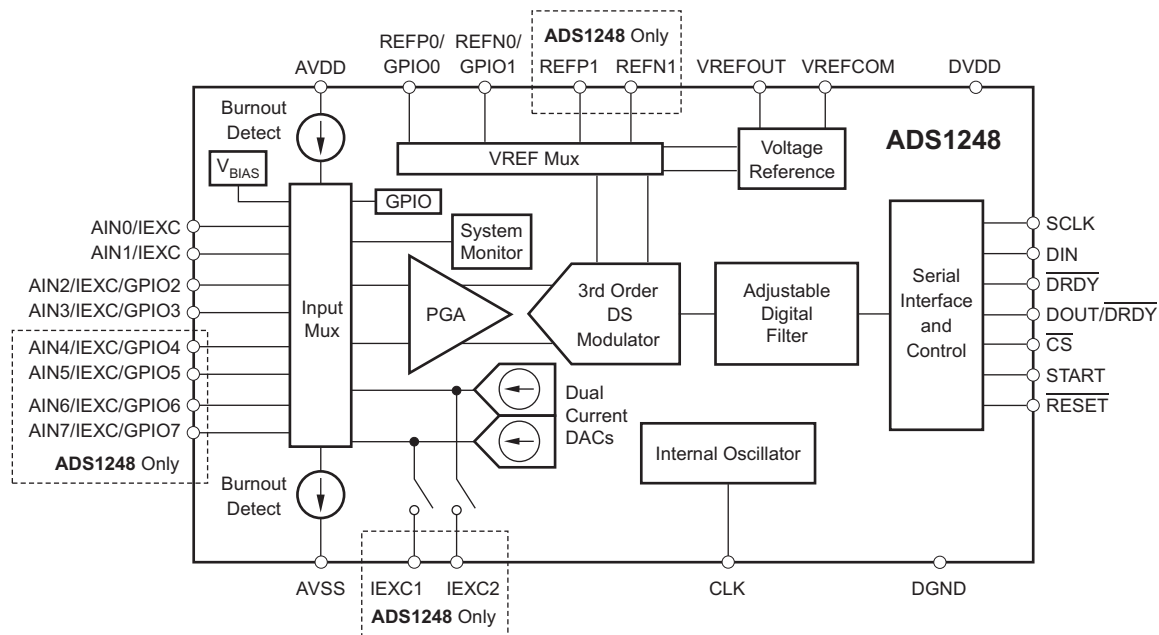


Figure 10. ADS1248 Block Diagram

4.1.3 TPS71745—Single Output LDO

Features:

- 150-mA low-dropout regulator with enable
- Low I_Q : 45 μ A (typical)
- Available in multiple output versions:
 - Fixed output with voltages from 0.9 to 5.0 V using innovative factory EEPROM programming
 - Adjustable output voltage from 0.9 to 6.2 V
- Ultra-high PSRR:
 - 70 dB at 1 kHz, 67 dB at 100 kHz, and 45 dB at 1 MHz
- Low noise: 30 μ V typical (100 Hz to 100 kHz)
- Stable with a 1.0- μ F ceramic capacitor
- Excellent load/line transient response
- 3% Overall accuracy (over load/line/temp)
- Overcurrent and over-temperature protection
- Very low dropout: 170 mV typical at 150 mA
- Small SC70-5, 2x2-mm SON-6, and 1.5x1.5-mm SON-6 packages

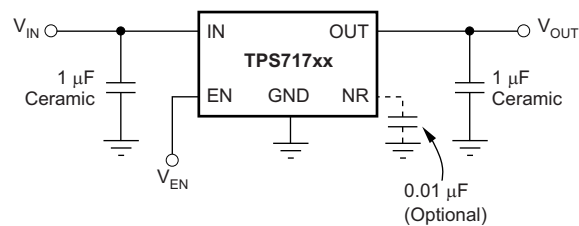


Figure 11. Typical Application Circuit for Fixed-Voltage Versions

5 Getting Started Hardware

To connect the TIDA-00564 BoosterPack, ensure that the connector index match on the LaunchPad and the BoosterPack.

Once connected, perform the following actions:

1. Connect the micro-USB of the LaunchPad to the PC.
2. Ensure in the Windows Device Manager (or alternative naming for other OS) that the board is recognized.
3. Install Energia™ if not yet done.
4. Load the sketch on the LaunchPad. For the sketch, contact a TI representative.
5. Open the serial monitor to display the read values.

5.1 LaunchPad Ecosystem

LaunchPads are microcontroller development kits from Texas Instruments focusing on ease of use for evaluation:

- Simple USB interface to PC (no more need for an additional debugger to connect to the JTAG port as the logic is already on the LaunchPad board)
- Standardized interface for extension boards (called BoosterPacks)

The LaunchPads comply with the following electrical interface specification, which is available as a pdf here: <http://www.ti.com/ww/en/launchpad/dl/boosterpack-pinout-v2.pdf>.

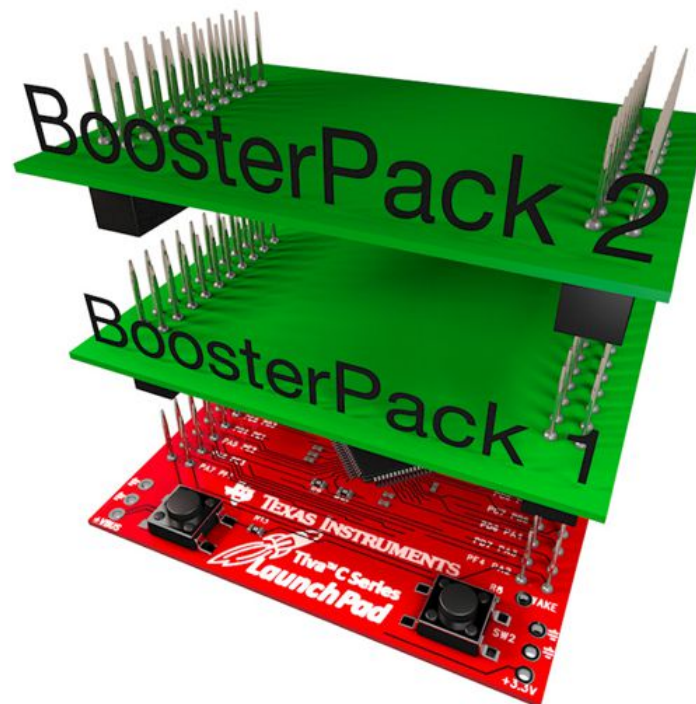


Figure 12. LaunchPad Ecosystem

5.1.1 BoosterPack

BoosterPacks are plug-in modules that fit on top of a LaunchPad. These innovative tools plug into a consistent and standardized connector on the LaunchPad and allow developers to explore different applications enabled by a TI microcontroller.

BoosterPacks are available from Texas Instruments, from third parties, and from the community. They include functions such as capacitive touch, wireless communication, sensor readings, LED lighting control, and more. BoosterPacks are available in 20- and 40-pin variants, and multiple BoosterPacks can plug into a LaunchPad to enhance the functionality of a design.

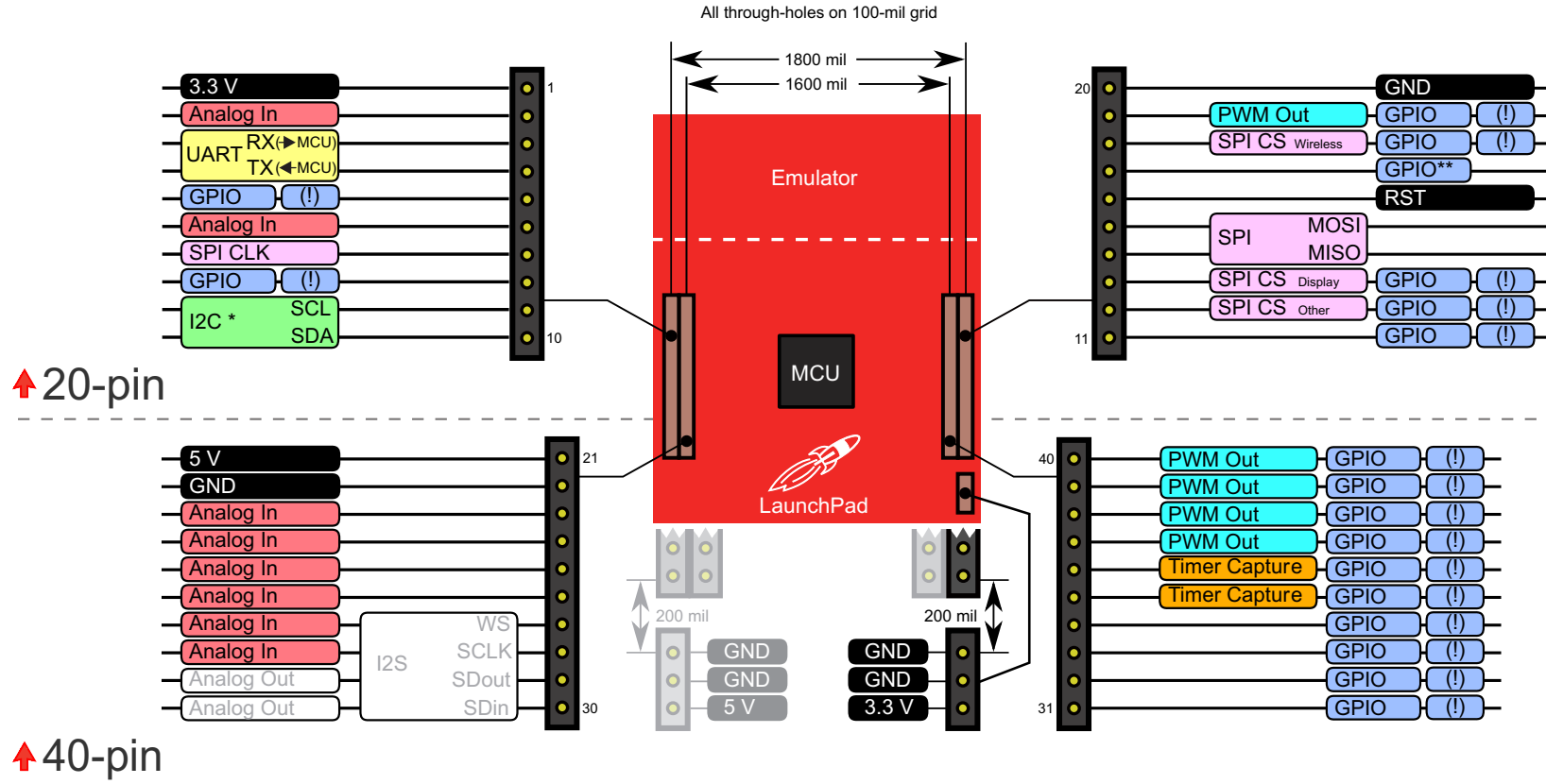


Figure 13. BoosterPack Pinout

6 Test Setup

For the room temperature test setup, the TIDA-00463 is always fixed in a certain position and the magnet moves backward and forward towards the board. For the over temperature test setup, both the TIDA-00463 and the magnet are fixed in a certain position.

At room temperature two test setups were implemented: one where the magnet moves in the same direction of the fluxgate axis, and one where it moves in a perpendicular direction with respect to the fluxgate axis.

6.1 Same Direction Test Setup

In this setup, the TIDA-00463 is fixed and the magnet moves in the same direction of the fluxgate axis (see Figure 14). The magnet in this setup is a 6-mm diameter NdFeB with $H_c > 1350$ kA/m.

The TIDA-00463 is connected to the LaunchPad, and this one is connected to any laptop where on a serial monitor are shown the acquired data. Energia code was implemented to configure the ADS1248 and to read back the data, sending them to the serial port.

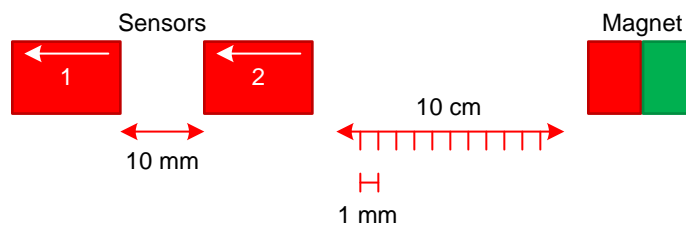


Figure 14. Same Direction Setup Scheme

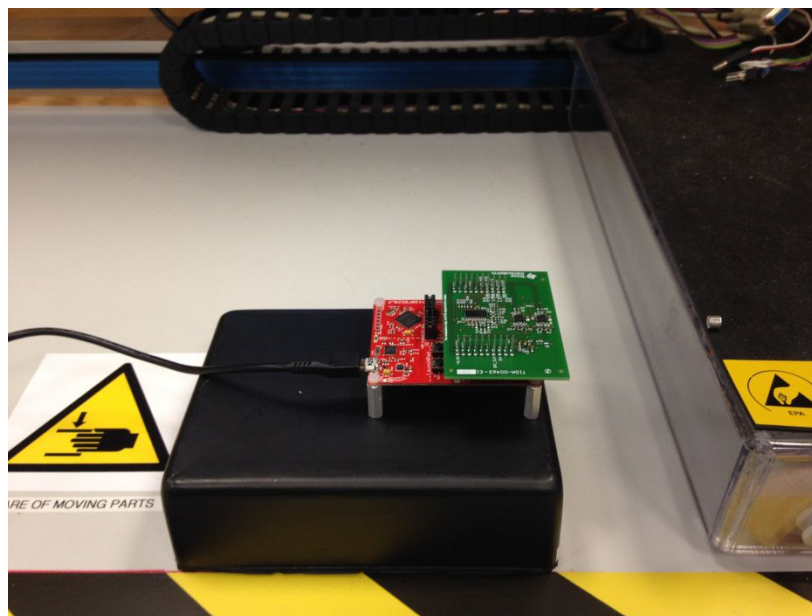


Figure 15. Same Direction Test Setup

6.2 Perpendicular Direction Test Setup

This setup is similar to the previous one with the only exception that the magnet moves in a perpendicular direction to the fluxgate axis (see Figure 16).

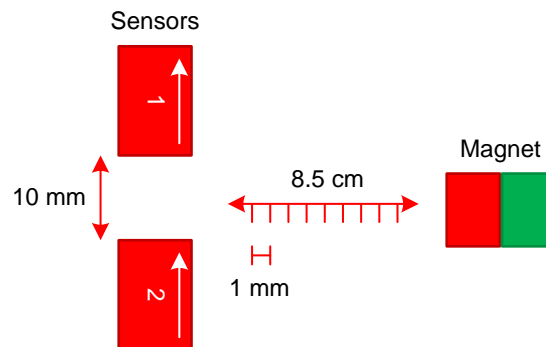


Figure 16. Perpendicular Direction Setup Scheme



Figure 17. Perpendicular Direction Test Setup

6.3 Over-Temperature Test Setup

To test over temperature, both the board and the magnet are in a fixed position. The distance of the magnet from the board is equal to 5 cm. Two temperature cycles are performed, one without a magnet in the oven and one with from -40°C up to 85°C .

Data acquisition happens in the same way of the first two test setups.

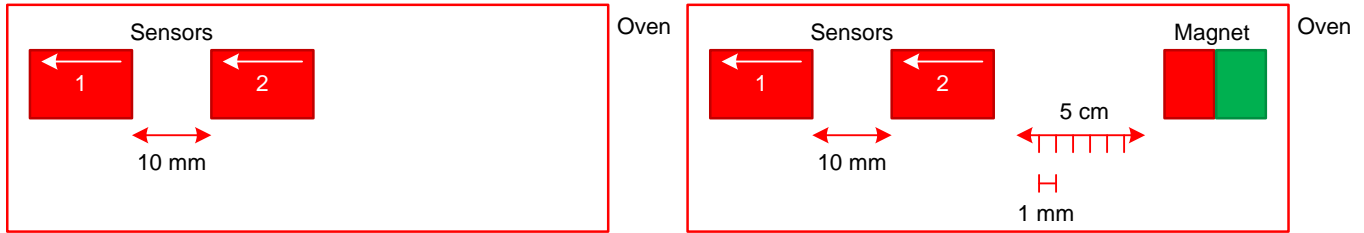


Figure 18. Over-Temperature Test Setup Scheme

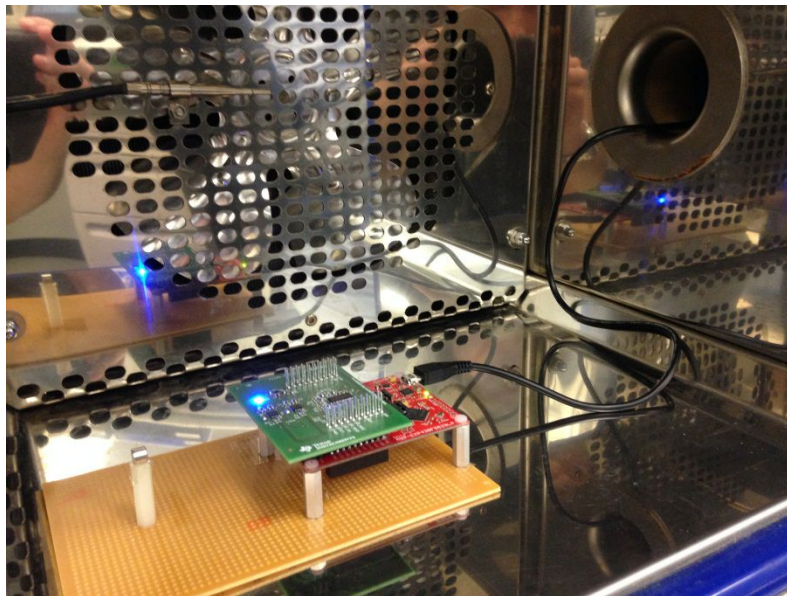


Figure 19. Over-Temperature Test Setup

7 Test Data

A first functional test without any magnet and at room temperature is performed to see if the board behaves as expected.

1000 measurements were acquired and the results plot in a histogram. The values on the x axis refer to the differential output voltage of the system in millivolt. Theoretically speaking, this should be zero because there is not a magnet around the board, so the only field present should be the common mode one—the earth magnetic field—and it should be cancelled by the differential measurement. However, there are some errors introduced by the fact that this design uses two different shunt resistors for the two devices, the manufacturer PCB tolerances that affect the alignment of the two fluxgates, and the 10-mm distance between the two sensors.

The average over 1000 samples of the measured differential output is equal to -7.39 mV ($-7.57\text{ }\mu\text{T}$) while the standard deviation equal to $21\text{ }\mu\text{V}$ (22 nT).

The average over 1000 samples of the measured single output voltage for the two DRV425 is equal to -25.43 mV for the first device and -32.84 mV for the second one, corresponding to $-26\text{ }\mu\text{T}$ and $-34\text{ }\mu\text{T}$, respectively. Note that this is the value of the earth magnetic field that ranges from ± 25 to $\pm 65\text{ }\mu\text{T}$. The maximum peak-to-peak noise measured is equal to $300\text{ }\mu\text{V}$ (320 nT). Considering that the chosen bandwidth of the DRV425 is around 30 kHz , the noise density according to the datasheet is $260\text{ nT}_{\text{RMS}}$. However, since the output of the system is the sum of the two DRV425 outputs, the total RMS noise is $368\text{ nT}_{\text{RMS}}$ ($260\text{ nT}_{\text{RMS}} \times \sqrt{2}$) and the peak-to-peak noise is five to six times the RMS noise (suitable value is 6.6 times the RMS value) equal to $2.43\text{ }\mu\text{T}$ (2.37 mV).

The measured peak-to-peak noise of the system is at least seven times lower than the estimated one of the two sensors, showing the good performances of the TIDA-00463.

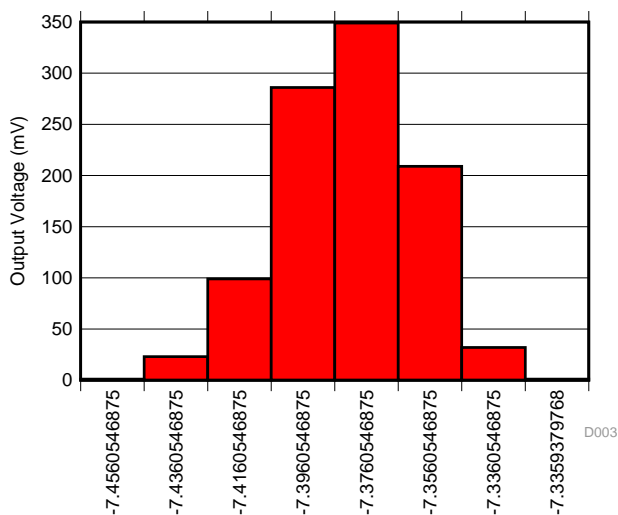


Figure 20. Measured Differential Output Voltage (mV)

7.1 Same Direction Test Data

As shown in Section 6.1, a magnet moves in 1-mm increments from 2 to 10 cm. 2 cm is the closest distance that the magnet can get to the board before the DRV425 closer to the TIDA-00463 edge saturates. After 10 cm, the resolution becomes smaller and smaller until 30 cm, after which the magnet is not detectable anymore. Note that with a bigger and stronger magnet, the measured distance becomes bigger.

In Figure 21, the black curve represents the output in μT of the sensor closer to the board edge, while the red curve represents the output of the other one. Notice how the two curves get closer as the distance increases, making the differential measurements of the two smaller. Figure 22 shows the differential output. Note that the resolution become bigger as the distance increases.

Figure 23 is a zoomed version of Figure 21 in the earth magnetic field range. It could be impossible to distinguish between the earth magnetic field and the actual magnetic field generated by the magnet if the differential output approach is not adopted (see Section 3.5) or without any calibration.

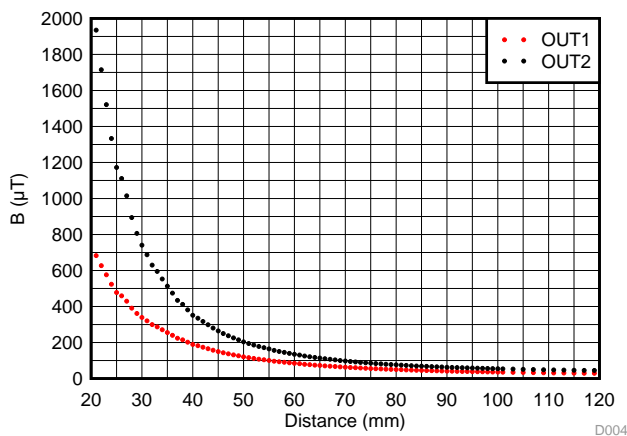


Figure 21. Measured Magnetic Field of Two DRV425 versus Distance

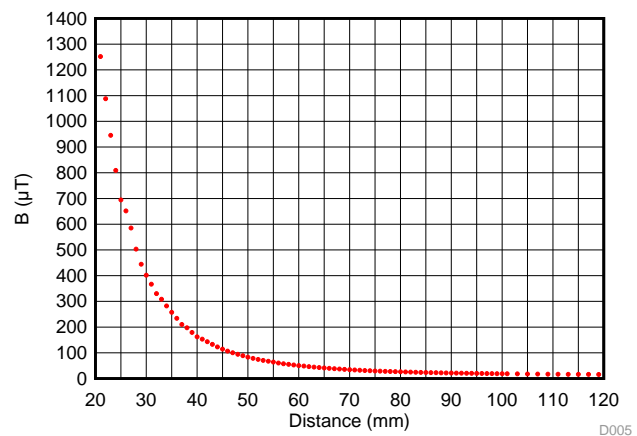


Figure 22. Differential Measured Magnetic Field versus Distance

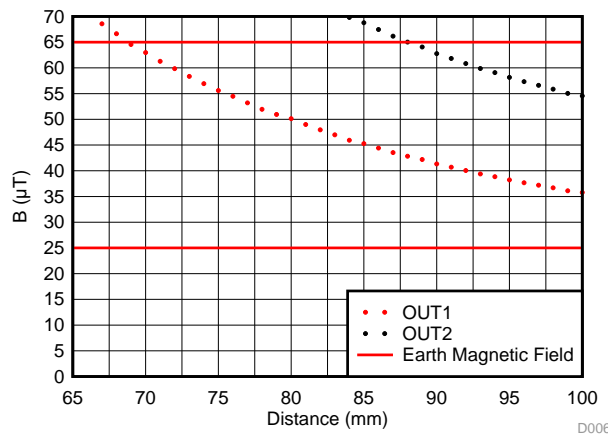


Figure 23. Measured Magnetic Field of Two DRV425 and Earth Magnetic Field versus Distance

7.2 Perpendicular Direction Test Data

In this test, the maximum reachable distance with a 1-mm resolution is 85 cm because the generated magnetic field hits the fluxgate direction perpendicularly, resulting in weaker results. The lowest measurable distance is 3.6 cm because of the board shape (see Figure 17) while the maximum one is around 25 cm, after which the magnet is not detectable anymore.

Note how the curves describe the magnetic field lines. If the main goal of the system is a large distance, this configuration is not recommended.

Everything else said in Section 7.1 is valid for this test as well.

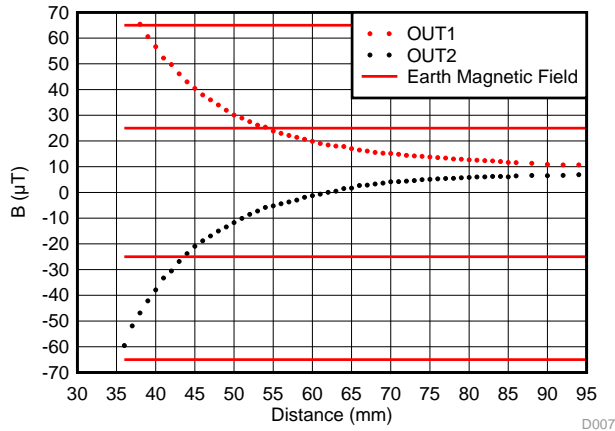


Figure 24. Measured Magnetic Field of Two DRV425 and Earth Magnetic Field versus Distance

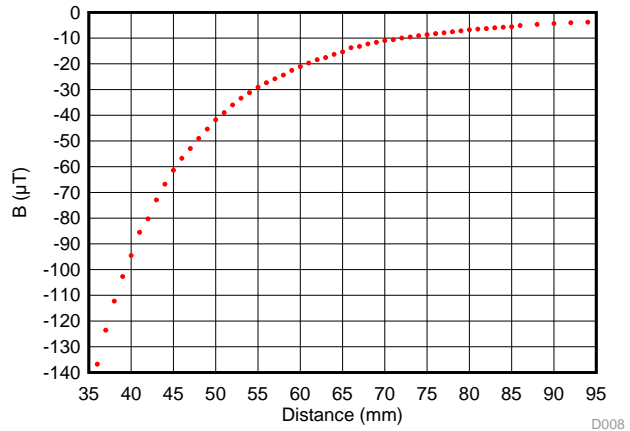


Figure 25. Differential Measured Magnetic Field versus Distance

7.3 Over-Temperature Test Data

1000 measurements were acquired for each temperature step (−40°C, 25°C, and 85°C) without any magnet and with the magnet placed 5 cm from the board. The first test setup measures over temperature.

A histogram is plotted for each temperature step and the standard deviation, mean, and maximum noise are calculated (see Table 3).

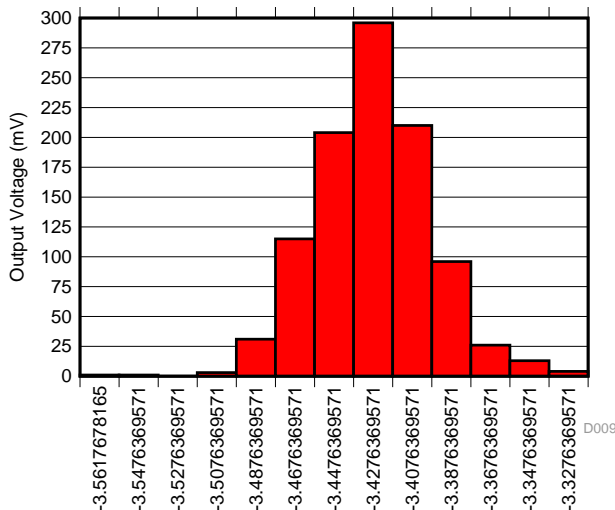


Figure 26. Differential Output (mV) Without Magnet Present at −40°C

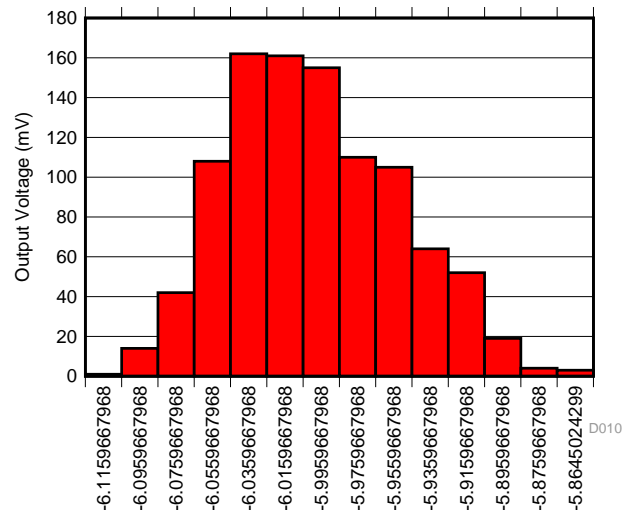


Figure 27. Differential Output (mV) Without Magnet Present at 25°C

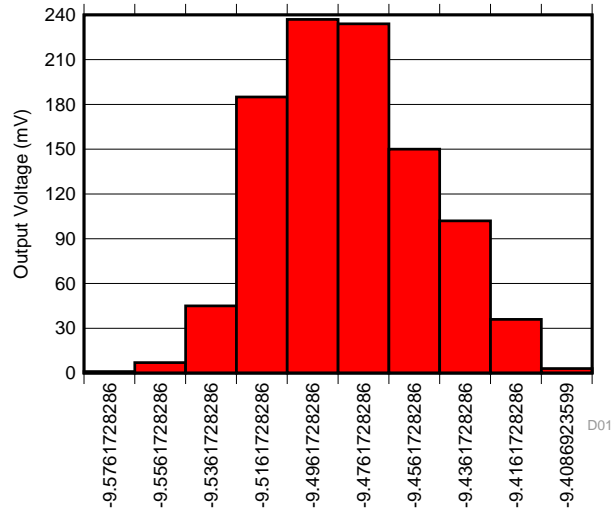


Figure 28. Differential Output (mV) Without Magnet Present at 85°C

Table 3. Over-Temperature Data Without Magnet

TEMPERATURE	STANDARD DEVIATION (μV)	MEAN (mV)	MAX NOISE [PEAK-TO-PEAK] (mV)
-40°C	30	-3.4	0.23
25°C	47	-6.0	0.25
85°C	30	-9.5	0.17

The maximum peak-to-peak noise measured is 0.25 mV (240 nT), a much lower value than the estimated one of the two sensors (see Section 7).

The temperature drift calculated as the mean value at 85°C minus the mean value at -40°C divided by the all temperature range is 50 $\mu\text{V}/^\circ\text{C}$ (52 nT/ $^\circ\text{C}$). This is due by many contributions: the temperature drift of the DRV425, TPS71745, and ADS1248, the temperature drift of the internal reference of the ADS1248, and the drift the shunt resistances value over temperature.

Figure 29 shows as the measured differential output change in function of the temperature.

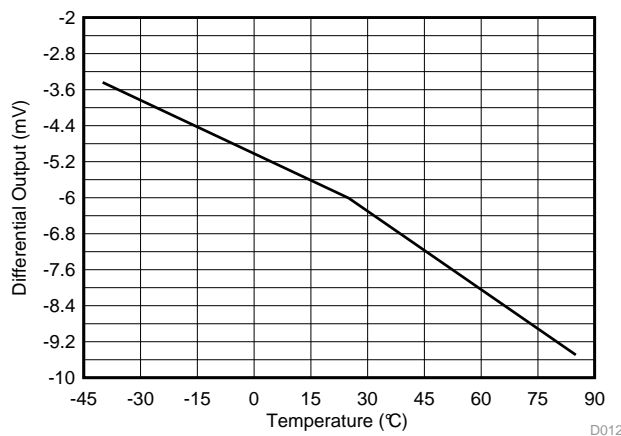


Figure 29. Measured Differential Output versus Temperature Without Magnet

The data obtained when the magnet is inside the oven 5 cm from the board are similar to the one obtained when it is not (see Table 4). The only difference in this case is that the temperature drift is the double (97 nT) because in this case it is influenced by the magnet changes over temperature. These results confirm that the system has good performances over temperature as well.

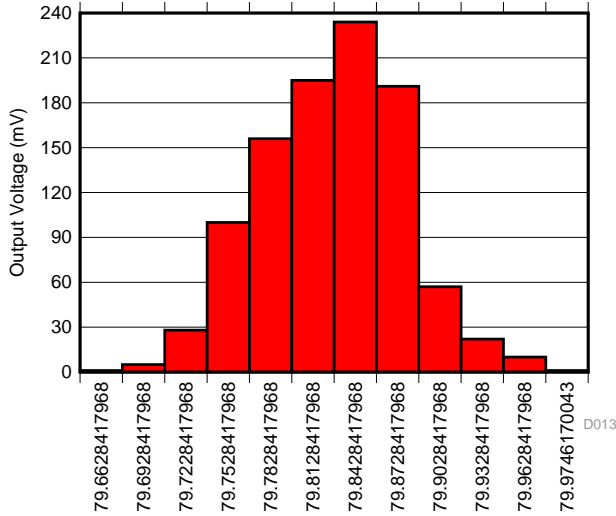


Figure 30. Differential Output (mV) When Magnet at 5 cm From DRV425 at -40°C

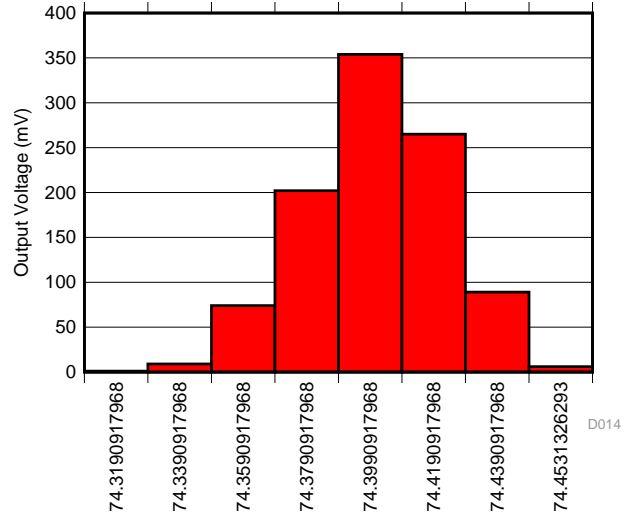


Figure 31. Differential Output (mV) When Magnet 5 cm From DRV425 at 25°C

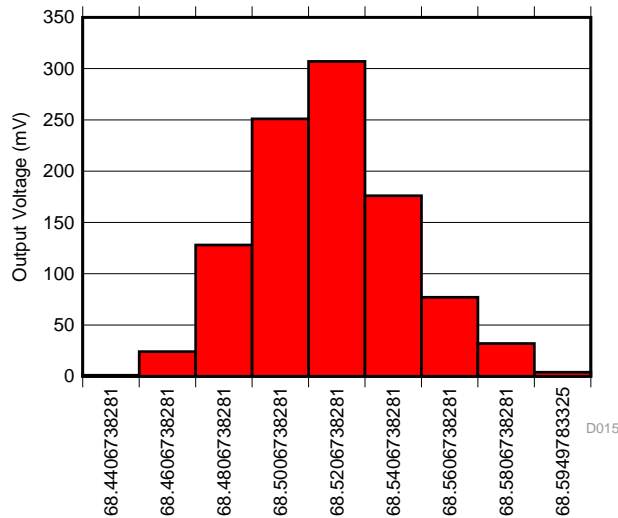
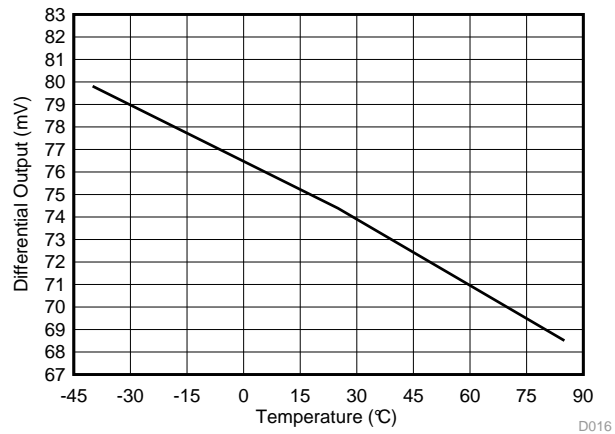


Figure 32. Differential Output (mV) When Magnet 5 cm From DRV425 at 85°C

Table 4. Over-Temperature Data With Magnet 5 cm From the Board

TEMPERATURE	STANDARD DEVIATION (μV)	MEAN (mV)	MAX NOISE [PEAK-TO-PEAK] (mV)
-40°C	50	79.80	0.31
25°C	22	74.39	0.13
85°C	26	68.50	0.15


Figure 33. Measured Differential Output versus Temperature When Magnet is 5 cm From DRV425

8 Design Files

8.1 Schematics

To download the schematics, see the design files at [TIDA-00463](https://www.ti.com/design-files/TIDA-00463).

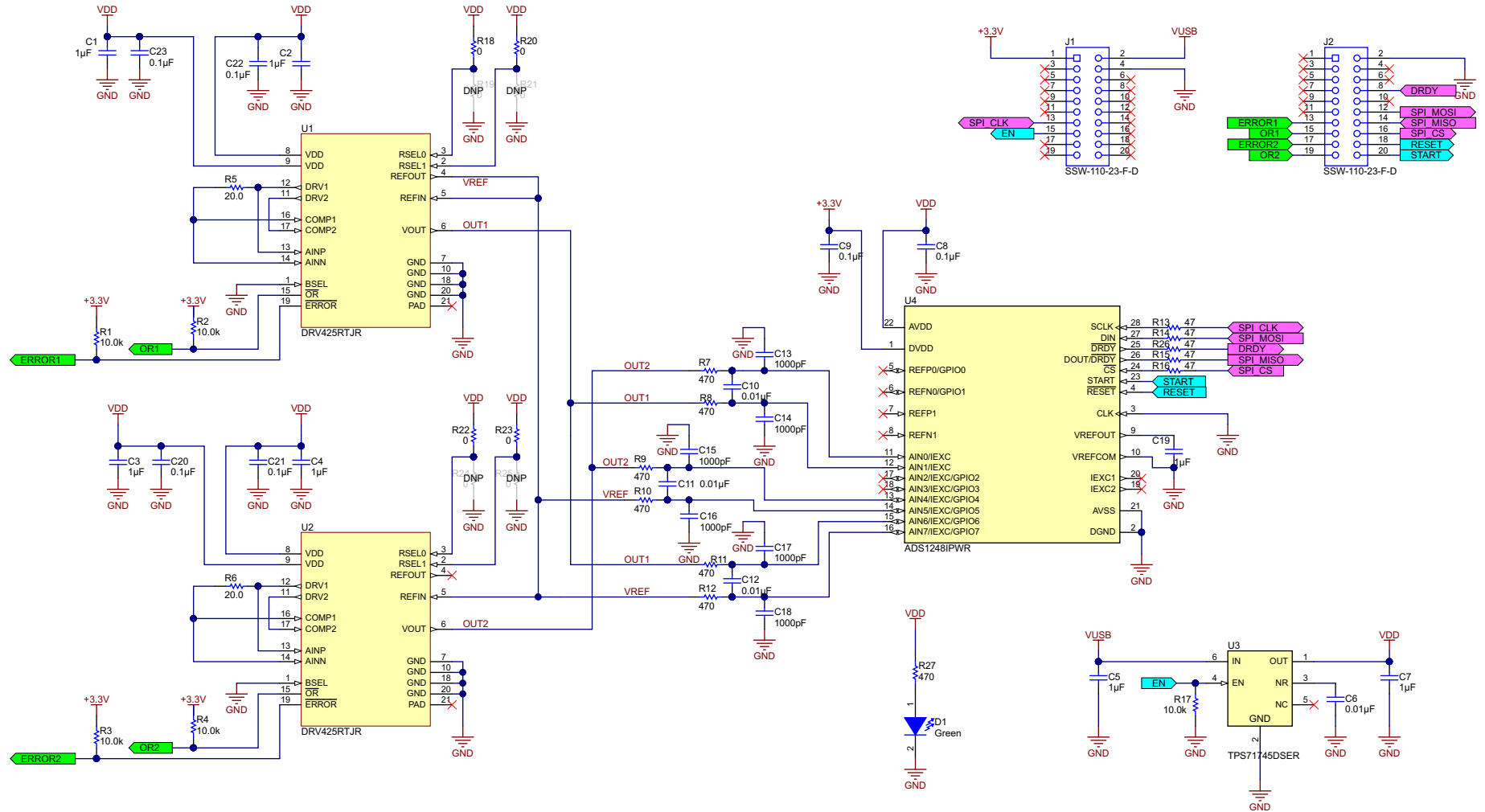


Figure 34. Fluxgate-Based Displacement Sensor Schematic

8.2 Bill of Materials

To download the bill of materials (BOM), see the design files at [TIDA-00463](#).

8.3 PCB Layout Recommendations

The board has been designed in a BoosterPack form factor:

- Place in a very precise way the two 20-pin connector at each side of the board so that they perfectly match with the 20-pin connector of the LaunchPad.
- For the DRV425 [9]:
 - Route current-conducting wires in pairs: route a wire with an incoming supply current next to, or on top of, its return current path. The opposite magnetic field polarity of these connections cancel each other. To facilitate this layout approach, the DRV425 positive and negative supply pins are located next to each other.
 - Route the compensation coil connections close to each other as a pair to reduce coupling effects.
 - Minimize the length of the compensation coil connections between the DRV1/2 and COMP1/2 pins.
 - Route currents parallel to the fluxgate sensor sensitivity axis. As a result, magnetic fields are perpendicular to the fluxgate sensitivity and have limited affect.
 - Vertical current flow (for example, through vias) generates a field in the fluxgate-sensitive direction. Minimize the number of vias in the vicinity of the DRV425.
 - Use nonmagnetic passive components (for example, decoupling capacitors and the shunt resistor) to prevent magnetizing effects near the DRV425.
 - Do not use PCB trace finishes with nickel-gold plating because of the potential for magnetization.
 - Connect all GND pins to a local ground plane.
 - Do not have a signal plane under the device.
- For the ADS1248 [11]:
 - Separate analog and digital signals. To start, partition the board into analog and digital sections where the layout permits. Route digital lines away from analog lines. This prevents digital noise from coupling back into analog signals.
 - The ground plane can be also split into an analog plane (AGND) and digital plane (DGND), but this is not necessary. Digital signals can be placed over the digital plane, and analog signals can be connected over the analog plane. As a final step in the layout, the split between the analog and digital grounds can be connected to together at the ADC.
 - Fill void areas on signal layers with ground fill.
 - Provide good ground return paths. Signal return currents will flow on the path of least impedance. If the ground plane is cut or has other traces that block the current from flowing right next to the signal trace, it will have to find another path to return to the source and complete the circuit. If it is forced into a larger path, that will increase the chances that the signal will radiate and that sensitive signals will be more susceptible to EMI.
 - Use high-frequency bypassing. Do not place vias between bypass capacitors and the active device. Placing the bypass capacitors on the same layer as and as close to the active device will yield the best results.
 - Consider the resistance and inductance of the routing. Often, traces for the inputs have a resistance that reacts with the input bias current and cause an added error voltage. Reducing the loop area enclosed by the source signal and the return current will reduce the inductance in the path. Reducing the inductance will reduce the EMI pickup and reduce the high frequency impedance seen by the device.
 - Watch for parasitic thermocouples in the layout, where dissimilar metals are used going from each input to the measurement. Differential inputs should be matched for both the inputs going to the measurement source.
 - Keep the reference impedances low.

- For the TPS71745:
 - Place all circuit components on the same side of the circuit board and as near as practical to the respective LDO pin connections.
 - Place ground return connections to the input and output capacitor, and to the LDO ground pin as close to the GND pin as possible, connected by wide, component-side, copper surface area.
 - Do not use vias and long traces to create LDO component connections, which negatively affects system performance. This grounding and layout scheme minimizes inductive parasitics, and thereby reduces load-current transients, minimizes noise, and increases circuit stability.
 - A ground reference plane is also recommended, which is either embedded in the printed circuit board (PCB) itself or located on the bottom side of the PCB opposite the components. This reference plane serves to assure accuracy of the output voltage, shields the LDO from noise, and functions similar to a thermal plane to spread (or sink) heat from the LDO device when connected to the thermal pad. In most applications, this ground plane is necessary to meet thermal requirements.

8.3.1 Layout Prints

To download the layout prints for each board, see the design files at [TIDA-00463](#).

8.4 Altium Project

To download the Altium project files, see the design files at [TIDA-00463](#).

8.5 Gerber Files

To download the Gerber files, see the design files at [TIDA-00463](#).

8.6 Assembly Drawings

To download the assembly drawings, see the design files at [TIDA-00463](#).

9 References

1. Ripka, Pavel, *Magnetic Sensor and Magnetometers*. Artech House Publishers (2001). ISBN: 978-1580530576.
2. Grüger, Heinrich, Angelika Grüger, and Florian Kaluza, *New and future applications of fluxgate sensors*. *J. Sensors, Sensor and Actuators A*, 10.6 (2003): 48–51.
3. Macintyre, Steven A., *Magnetic Field Measurement*. CRC Press, 1999 ([PDF](#)).
4. Ripka, Pavel, *Advances in Magnetic Fluxgate Sensors*, 10.6 (2010): 1108–1116 ([PDF](#)).
5. Evans, Ken, *Fluxgate Magnetometer Explained*, (2006; [PDF](#)).
6. Suitella, Dominggus Yosua and Dr. Ir. Djoko Windarto, MT, *High Precision Fluxgate Current Sensor*, (2011; [PDF](#)).
7. Meeker, D.C., FEMM 4.2, *Finite Element Method Magnetics*. <http://www.femm.info> [Accessed on 09/08/2014].
8. Larson, Mats G. and Fredrik Bengzon, *The Finite Element Method: Theory, Implementation, and Applications*. Texts in Computational Science and Engineering. Berlin, Heidelberg: Springer, (2013). ISBN: 978-3-642-33287-6.
9. Texas Instruments, *DRV425 Fluxgate Magnetic-Field Sensor*, DRV425 Datasheet ([SBOS729](#)).
10. Texas Instruments, *TPS717xx Low-Noise, High-Bandwidth PSRR, Low-Dropout, 150-mA Linear Regulator*, TPS71745 Datasheet ([SBVS068](#)).
11. Texas Instruments, *24-Bit Analog-to-Digital Converters for Temperature Sensors*, ADS1248 Datasheet ([SBAS426](#)).
12. Lenz, James and Alan S. Edelstein, *Magnetic sensors and their applications*. *IEEE Sensors Journal*, 6.3 (2006): 631–649 ([PDF](#)).

10 About the Author

GIOVANNI CAMPANELLA is an Industrial Systems Engineer with the Field Transmitter Team in the Factory Automation and Control organization. He earned his bachelor's degree in electronic and telecommunication engineering at the University of Bologna and his master's degree in electronic engineering at the Polytechnic of Turin in Italy. His design experience covers sensors and analog signal chain (with a focus on fluxgate and analytics sensing technologies) and mixed-signal control of DC-brushed servo drives.

IMPORTANT NOTICE FOR TI REFERENCE DESIGNS

Texas Instruments Incorporated ("TI") reference designs are solely intended to assist designers ("Buyers") who are developing systems that incorporate TI semiconductor products (also referred to herein as "components"). Buyer understands and agrees that Buyer remains responsible for using its independent analysis, evaluation and judgment in designing Buyer's systems and products.

TI reference designs have been created using standard laboratory conditions and engineering practices. **TI has not conducted any testing other than that specifically described in the published documentation for a particular reference design.** TI may make corrections, enhancements, improvements and other changes to its reference designs.

Buyers are authorized to use TI reference designs with the TI component(s) identified in each particular reference design and to modify the reference design in the development of their end products. HOWEVER, NO OTHER LICENSE, EXPRESS OR IMPLIED, BY ESTOPPEL OR OTHERWISE TO ANY OTHER TI INTELLECTUAL PROPERTY RIGHT, AND NO LICENSE TO ANY THIRD PARTY TECHNOLOGY OR INTELLECTUAL PROPERTY RIGHT, IS GRANTED HEREIN, including but not limited to any patent right, copyright, mask work right, or other intellectual property right relating to any combination, machine, or process in which TI components or services are used. Information published by TI regarding third-party products or services does not constitute a license to use such products or services, or a warranty or endorsement thereof. Use of such information may require a license from a third party under the patents or other intellectual property of the third party, or a license from TI under the patents or other intellectual property of TI.

TI REFERENCE DESIGNS ARE PROVIDED "AS IS". TI MAKES NO WARRANTIES OR REPRESENTATIONS WITH REGARD TO THE REFERENCE DESIGNS OR USE OF THE REFERENCE DESIGNS, EXPRESS, IMPLIED OR STATUTORY, INCLUDING ACCURACY OR COMPLETENESS. TI DISCLAIMS ANY WARRANTY OF TITLE AND ANY IMPLIED WARRANTIES OF MERCHANTABILITY, FITNESS FOR A PARTICULAR PURPOSE, QUIET ENJOYMENT, QUIET POSSESSION, AND NON-INFRINGEMENT OF ANY THIRD PARTY INTELLECTUAL PROPERTY RIGHTS WITH REGARD TO TI REFERENCE DESIGNS OR USE THEREOF. TI SHALL NOT BE LIABLE FOR AND SHALL NOT DEFEND OR INDEMNIFY BUYERS AGAINST ANY THIRD PARTY INFRINGEMENT CLAIM THAT RELATES TO OR IS BASED ON A COMBINATION OF COMPONENTS PROVIDED IN A TI REFERENCE DESIGN. IN NO EVENT SHALL TI BE LIABLE FOR ANY ACTUAL, SPECIAL, INCIDENTAL, CONSEQUENTIAL OR INDIRECT DAMAGES, HOWEVER CAUSED, ON ANY THEORY OF LIABILITY AND WHETHER OR NOT TI HAS BEEN ADVISED OF THE POSSIBILITY OF SUCH DAMAGES, ARISING IN ANY WAY OUT OF TI REFERENCE DESIGNS OR BUYER'S USE OF TI REFERENCE DESIGNS.

TI reserves the right to make corrections, enhancements, improvements and other changes to its semiconductor products and services per JESD46, latest issue, and to discontinue any product or service per JESD48, latest issue. Buyers should obtain the latest relevant information before placing orders and should verify that such information is current and complete. All semiconductor products are sold subject to TI's terms and conditions of sale supplied at the time of order acknowledgment.

TI warrants performance of its components to the specifications applicable at the time of sale, in accordance with the warranty in TI's terms and conditions of sale of semiconductor products. Testing and other quality control techniques for TI components are used to the extent TI deems necessary to support this warranty. Except where mandated by applicable law, testing of all parameters of each component is not necessarily performed.

TI assumes no liability for applications assistance or the design of Buyers' products. Buyers are responsible for their products and applications using TI components. To minimize the risks associated with Buyers' products and applications, Buyers should provide adequate design and operating safeguards.

Reproduction of significant portions of TI information in TI data books, data sheets or reference designs is permissible only if reproduction is without alteration and is accompanied by all associated warranties, conditions, limitations, and notices. TI is not responsible or liable for such altered documentation. Information of third parties may be subject to additional restrictions.

Buyer acknowledges and agrees that it is solely responsible for compliance with all legal, regulatory and safety-related requirements concerning its products, and any use of TI components in its applications, notwithstanding any applications-related information or support that may be provided by TI. Buyer represents and agrees that it has all the necessary expertise to create and implement safeguards that anticipate dangerous failures, monitor failures and their consequences, lessen the likelihood of dangerous failures and take appropriate remedial actions. Buyer will fully indemnify TI and its representatives against any damages arising out of the use of any TI components in Buyer's safety-critical applications.

In some cases, TI components may be promoted specifically to facilitate safety-related applications. With such components, TI's goal is to help enable customers to design and create their own end-product solutions that meet applicable functional safety standards and requirements. Nonetheless, such components are subject to these terms.

No TI components are authorized for use in FDA Class III (or similar life-critical medical equipment) unless authorized officers of the parties have executed an agreement specifically governing such use.

Only those TI components that TI has specifically designated as military grade or "enhanced plastic" are designed and intended for use in military/aerospace applications or environments. Buyer acknowledges and agrees that any military or aerospace use of TI components that have **not** been so designated is solely at Buyer's risk, and Buyer is solely responsible for compliance with all legal and regulatory requirements in connection with such use.

TI has specifically designated certain components as meeting ISO/TS16949 requirements, mainly for automotive use. In any case of use of non-designated products, TI will not be responsible for any failure to meet ISO/TS16949.